Centrifugal Etching: A Promising New Tool to Achieve Deep Etching Results

H. K. Kuiken and R. P. Tijburg

Philips Research Laboratories, 5600 JA Eindhoven, The Netherlands

ABSTRACT

This paper presents some theoretical considerations to show that by etching in an enhanced acceleration field, such as can be obtained in a centrifuge, it is possible to circumvent many of the typical objectionable features of some of the traditional etching techniques. The theory is corroborated by a small series of experiments. These clearly indicate that centrifugal etching may yield very low undercutting, large etch rates, and, if proper care is taken, an extremely smooth surface finish.

In many etching processes, the diffusional transport of the active components of the etchant to the surface or of the etched materials away from the surface, is a factor that severely limits the etch rate. The reason is that the diffusion coefficient of species dissolved in liquids is very small. D is of the order of 10^{-9} m²/sec (1), but it may be greater than that number depending upon the temperature. To increase the etch rate, various methods, such as jet, spray, or film etching, are used. The common feature of these methods is that the etchant is forced to flow along the surface, thus adding the effect of convectional transport. If the purpose of the etching procedure is to produce small holes or slits in an otherwise smooth surface, the flow will almost never directly penetrate into the holes (2). Except when the cavity is shallow, the etchant moves along the hole, the flow in the cavity being characterized by one or more trapped eddies. It has been shown before (3) that the transport of reactants or of reaction products often occurs in a thin boundary layer that exists along the rim of the vortex. The exchange of etching products occurs by means of diffusion across the streamline that separates the eddies from one another or from the outer flow (Fig. 1).

Although adding convection will certainly increase the etch rate, etching methods that involve the forcing of the etchant along the hole pattern have one inherent drawback. It has, in fact, been shown experimentally (4) and explained theoretically (3) that the emergence of every new vortex leads to a drastic reduction of the etch rate (Fig. 2). This results in strong undercutting effects. In any case, it is doubtful whether, in the end, the etch depth will ever be much larger than the final hole width. Therefore, deep etching using forced flow outside the holes is probably impossible. This is also borne out by the experiments performed by Allen et al. (5-8). When convection effects are excluded, i.e., in purely diffusional processes, deep etching with respect to hole diameter in isotropic materials is equally impossible. Indeed, in such materials a diffusion process does not have a characteristic direction, and eventually etching will result in almost spherically shaped cavity walls.

The purpose of this paper is to propose an alternative method of etching that does involve convection but circumvents the deleterious side effects mentioned

above. This method makes use of the fact that in an actual etching process, the density of the liquid certainly is not uniform throughout the system. In many instances, the fluid will become more dense if reaction products are added to it. This means that in such cases the fluid close to the wall of the cavity is more dense than the remaining pure etchant. When the complete system is put in an acceleration field, e.g., inside a centrifuge or in the ordinary gravity field, and care is taken to ensure that the acceleration vector is pointing out of the hole, the more dense "polluted" fluid will be drawn out, thus creating a natural convection pattern inside the cavity. Now there will be no trapped vortex within the cavity of the kind sketched in Fig. 1, as the fluid flows outward along the wall and, by the requirement of continuity, inward through the center (Fig. 3). It should be realized that pure etchant now first encounters the bottom of the cavity, thereby creating the largest etch rate exactly where it is needed. The impurity level grows along the side walls in the upward direction which results in lower etch rates closer to the orifice. It would seem that, by using this method, deep levels of penetration can be reached and that undercutting can be kept to a minimum.

It is obvious that the acceleration vector should point inward when addition of dissolution products to the etchant leads to lower densities. This is equally true if the removal of active species leads to an etchant of lower density. The acceleration vector should also point inward when the heat produced during the etching process is so large that thermal expansion exceeds the density enhancement due to the addition of etching products. If it is difficult to assess the relative magnitude of these two effects by theoretical means, suitable experiments will be needed in order to decide how to apply the acceleration field.

In the remaining part of this paper, we discuss some of the theoretical ideas that explain how natural convection can be an effective means of transporting reactants into and reaction products out of a cavity. Several experiments were carried out using a centrifuge, and we present some of the results in this paper. To simplify the presentation, we assume an etching process in which the "polluted" etchant has a higher density than pure etchant. As was explained above, the other cases can be dealt with similarly.
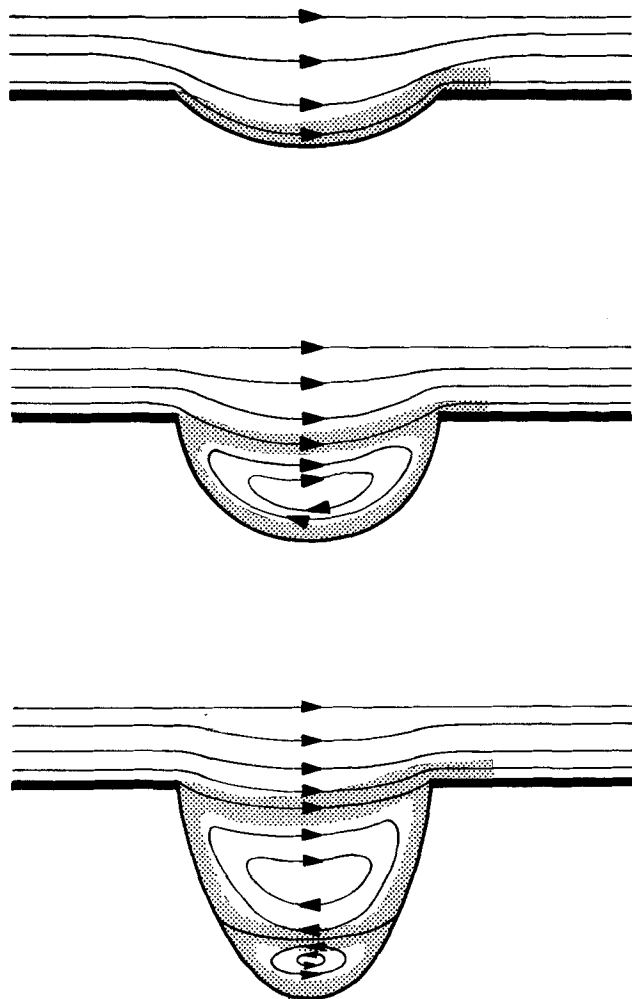
Fig. 1. Qualitative picture of mass transfer from an open cavity as a function of cavity depth in jet etching. Arrows denote flow direction. Reaction products occupy the dotted regions.
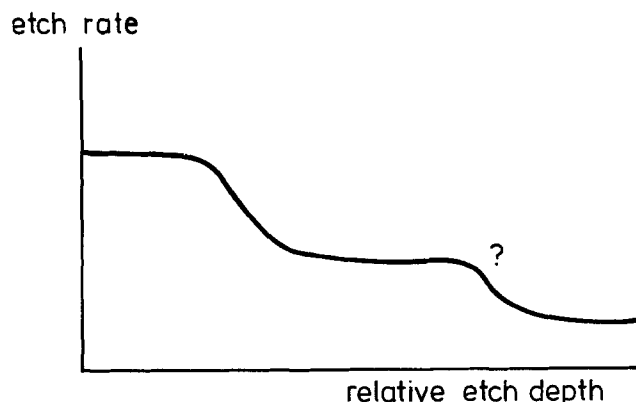

Fig. 2. Qualitative picture of etch rate as a function of etch depth in jet etching. Dips are caused by the emergence of new cells in the flow pattern. The question mark signifies that due to under-cutting the two-cell pattern may never arise in practice.
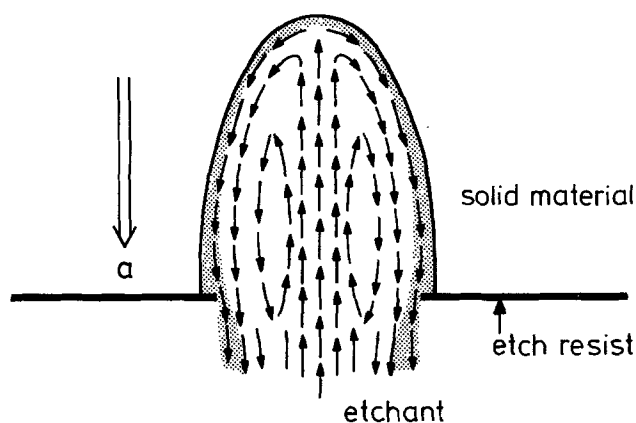

Fig. 3. Mass transfer from a cavity with free convective stirring. Arrows denote the direction of flow. Reaction products occupy the dotted region. The acceleration field is denoted by a. Case depicted assumes that reaction products are heavier than pure etchant.

Theoretical Considerations

In order that we may decide whether natural convection of the type described in the above section can really contribute to the transport of etched materials in an actual situation, we must have an estimate of the relative magnitudes of convectional and diffusional transport. In a standing etchant, i.e., when stirring is absent, the transport of reaction products is due solely to diffusion down a concentration gradient. Therefore, the convective transport due to free convective stirring should at least be as large as the diffusional transport component, if it is to be noticeable at all.

Clearly, free convective stirring will be useful only if it dominates convection. In a system that is characterized by a large Schmidt number

$$Sc = \nu/D \qquad [1]$$

where ν is the kinematic viscosity of the etchant ($\sim 10^{-6}$ m^2/sec) and D is the diffusion coefficient ($\sim 10^{-9}$ m^2/sec), it is essentially the Rayleigh number (Ra)

$$Ra = a\beta(\Delta c)l^3/(\nu D) \qquad [2]$$

that determines the relative importance of convection and diffusion (9). In Eq. [2], a denotes the acceleration field (m/sec^2) and l is a length (m) that is characteristic for the size of the system. At the start of the etching process, l may be taken as the half-width of the etchable area. When a deep hole has been etched, the depth may be taken as the characteristic length. Further, Δc is a measure of the concentration

difference (mol/m^3) of the reaction products, and β is the coefficient of volumetric expansion. In actual fact, if the density variations are not too large, the density of the polluted etching fluid can be given by the linear relationship

$$\rho = \rho_0(1 + \beta\Delta c) \qquad [3]$$

where ρ_0 is the density of pure etchant. Should thermal effects be important (reaction heat), Eq. [3] will have to be extended to include these

$$\rho = \rho_0(1 + \beta\Delta c - \beta_H\Delta T) \qquad [4]$$

where T is the temperature and β_H signifies the coefficient of thermal expansion.

Convection effects are dominant if the Ra number is considerably larger than unity. It is known, from both the heat and the mass transfer literature (10, 11), that Ra should at least be on the order of one hundred for convection really to dominate over diffusion. To obtain an idea of the values Ra may assume, consider what happens in an ordinary gravity field ($a = 10$ m/sec^2), using the values of D and ν already given. If the cavity to be etched has an original width of 100 μm, we have $l \sim \frac{1}{2} \cdot 10^{-4}$m (half-width). A reasonable value of $\beta\Delta c$ would seem to be 0.01, which means a density change on the order of one percent. Ra for this case is about 10, which seems to be too small for convection to have a significant influence on the etching process.

To obtain large etching rates in the example cited above, we might employ what may be called an artificial gravity field that can be created inside a centri-

fuge. Values of a up to 10^4 m/sec^2 can be created even in a simple centrifuge. Using such an apparatus, we may induce an intense natural-convective stirring right from the start of the process. In the example given above, the Ra number would be on the order of 10^4 at least, ensuring the dominance of natural convection over pure diffusion.

When the holes to be etched become smaller, the Ra number decreases in proportion to the third power of the characteristic length. Therefore, when etching smaller holes, leaving all other parameters in the system unchanged, we eventually have to use a more powerful ultracentrifuge (larger a) to keep the Ra number at high levels.

Further, it should be remarked that in Ra-number-determined flows, cellular flow patterns may emerge. These are called Bénard cells, which emerge when the fluid density gradient and the external field are parallel but directed oppositely. An array of such cells is sketched in Fig. 4, together with the etching pattern that may be expected on account of these cells. Later in this paper, we consider this phenomenon in more detail to explain certain experimental results.

To conclude this section, we devote some attention to the possible Sherwood numbers (Sh) that can be obtained through centrifugal etching. Here the Sh number is defined by

$$Sh = \phi L / (D \Delta c) \qquad [5]$$

where ϕ is the flux of dissolved product and L is a length that characterizes the size of the active surface, *e.g.*, the hydraulic radius. To get an insight into the possible values Sh may attain, we appeal to the results obtained for free-convective mass transfer at horizontal electrodes (12). If Ra is in the range $3 \times 10^4 < Ra < 2.5 \times 10^7$, we have

$$Sh = 0.64 \, Ra^{1/4} \qquad [6]$$

Although it is not explicitly stated in (12), it would seem that both Ra and Sh in Eq. [6] are based on the width L of the mass transfer area.

The Ra range of validity of Eq. [6] is restricted by the transition to turbulent flow (upper bound) and the inaccuracies of laminar boundary-layer theory at smaller Ra numbers (lower bound). The results of Goldstein *et al.* (13) are very useful to determine the Sh number in the lower Ra range. The correlations established by these authors are

$$Sh = 0.59 \, Ra^{1/4} \quad (Ra > 200) \qquad [7a]$$

$$Sh = 0.96 \, Ra^{1/6} \quad (Ra < 200) \qquad [7b]$$

It should be noted that the characteristic length used in Eq. [7a] and [7b] is determined by dividing the area of the mass transfer region by its perimeter. For long stripes, this means that the half-width should be taken. On the other hand, for circular or square regions the quarter-diameter and the quarter-width should be used respectively.

It is tempting to compare the Sh-Ra correlations of Eq. [6] and [7] with those referring to forced convection flows that prevail in jet etching. The appropriate Sh-Sc-Re correlation depends strongly upon the way in which the etchant is forced onto and along the surface. Reference (9) presents some of these correlations which show that for $Ra = 10^4$, the Sh numbers that follow from Eq. [6] or [7] are an order of magnitude smaller than the corresponding forced convection ones. However, as the holes become deeper, the forced convection Sh numbers will rapidly drop to lower values for reasons discussed before (see discussion of Fig. 1). The natural-convective correlations, on the other hand, will remain valid. Since free convection along vertical surfaces is more effective in terms of mass transfer rates, the free-convective Sh numbers may even go up a little bit as soon as a vertical sidewall of a length comparable to the hole width has been developed during the etching process.

Experimental

A beaker containing the etchant was placed in a centrifuge with a maximum rotation rate of 30 rps, which gave an artificial gravity of $+$ or $-$ 500g at the location of the test samples. The apparatus we used was a simple table centrifuge that was originally designed for the spin drying of silicon wafers.

The samples were mounted on the top or the bottom surface of a glass holder along which the etchant could flow freely. During spinning, samples mounted on the top of the holder experienced a positive, *i.e.*, inward directed artificial gravity with respect to the test pattern surface, whereas samples fixed to the bottom surface were subject to a negative (outward directed) gravity at the test pattern surface. A schematic picture of the experimental setup is given in Fig. 5.

A single experiment ($\pm 25{,}000$g) was carried out in an ultracentrifuge. In the latter experiment, we used a Teflon sample holder, the shape and the size of which
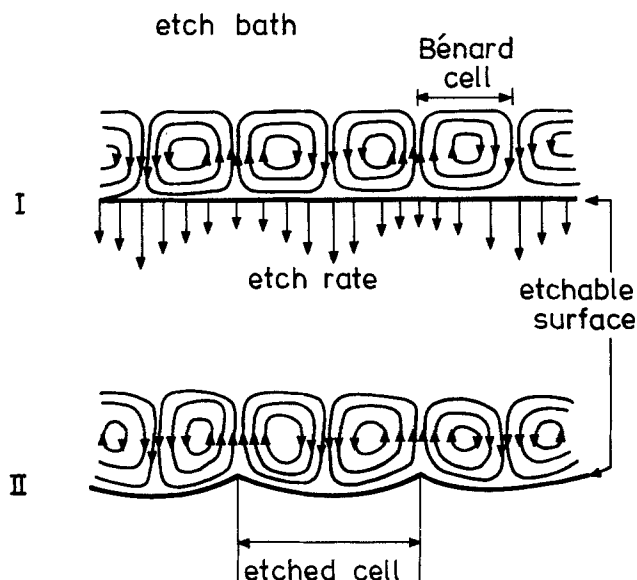
Fig. 4. Bénard cell flow pattern and resulting etching structure. (I) Initial flow pattern and etch rate distribution. (II) Sketch typifying a later stage of the etching process.
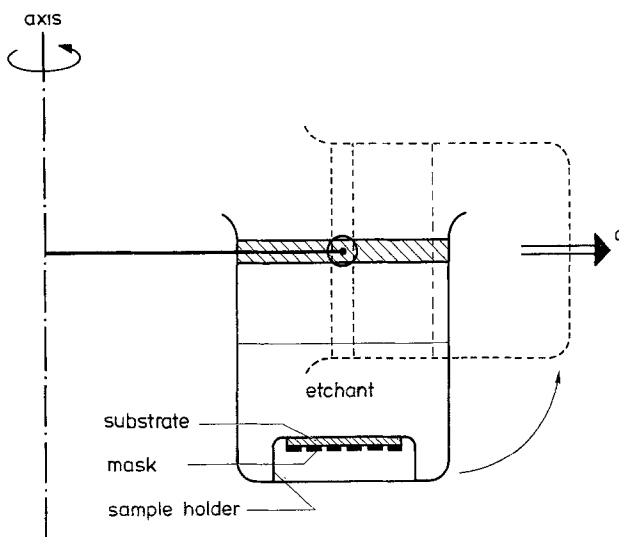
Fig. 5. Apparatus used in centrifugal etching. Case depicted refers to negative artificial gravity. The acceleration field is denoted by *a*.

were adapted to the special elongated beakers employed in an ultracentrifuge of the swing-out type. Again, this kind of centrifuge was not specially designed for etching purposes, as it is used extensively for biological sedimentation experiments.

In order to investigate whether the theoretical considerations presented earlier in this paper are valid, we took as test samples monocrystalline (1,0,0) oriented n-type GaAs slices as well as magnesium-bronze sheets both with thicknesses of 200 and 400 μm. We used a test pattern of circles with diameters ranging from 80 to 5000 μm. The etch resistant layer on GaAs was pyrolitic SiO_2 and on bronze the so-called C lacquer.[1]

The GaAs slices were etched either with a preferential or a nonpreferential etchant. The former is very sensitive to crystallographic orientation, and the etchant used (3,1,1) exhibits the lowest etch rate on (1,1,1) surfaces.

3 vol parts CH_3OH (methanol)
1 vol part H_3PO_4 (conc)
1 vol part H_2O_2 (30%)

The nonpreferential etchant (5,5,2) had the following composition

5 vol parts H_3PO_4 (conc)
5 vol parts H_2SO_4 (conc)
2 vol parts H_2O_2 (30%)

At the start of the experiment, the temperature of the etchant was 20°C.

Results

In Table I, results with GaAs pertaining to the etched depths have been summarized. The circular areas had large diameters compared to the etched depths. It should be noted that the nonpreferential etchant yields an extremely smooth surface finish (Fig. 6).

Sheets of bronze were etched in a centrifuge in aqueous solutions of $FeCl_3$ with s.w. 1.40 g/cm³ and with an artificial gravity ranging from + 500 to − 25,000g. Results obtained from experiments in which the artificial gravity was directed away from the test pattern surface, as well as those where the artificial gravity was directed inward, seem to confirm some of the theoretical expectations.

When the gravity field was directed toward the test pattern, the etched holes, with diameters ranging from 80 to 5000 μm have perpendicular sidewalls and flat bottom surfaces. There is no evidence of Bénard cell structures which are characteristic for the negative gravity case (see below). The undercutting amounted to about one-half of the etched depth for etching times of up to 15 min. For longer etching times, it tends to become equal to the etched depth. With the conditions described in Table II for the − 350g experiment, the + 350g experiment showed etching depths of approximately 40 and 50 μm for etching times of 15 and 30 min, respectively. After 90 min of etching, the holes were rather deformed with a maximum depth of about 100 μm.

With the gravity field directed away from the test pattern surface, we used accelerations of − 140, − 350,

[1] A polyvinylbutyral-based negative lacquer (made by Philips for internal use).

Fig. 6. Smooth surface finish in GaAs (+350g); 70°C; 30 sec; etch bath 3:1:1 (H_2SO_4:H_2O_2:H_2O).

−500, and −25,000g. To achieve the largest of these values, we used an ultracentrifuge in a single experiment. Apart from the etching time, the depths of the holes obtained depend on the artificial gravity and on original hole diameter. Since the thickness of the bronze sheet used was not more than 400 μm, holes which otherwise would have been deeper could not be measured. The lower values given in Table II refer to holes with a diameter of 100 μm.

The 5000 μm hole shows an exception to this rule, as the average etch rate drops continually; we attribute this unusual behavior to a temperature effect. In Table III, results are given for various etching times and hole diameters. Starting at a rather high value, the etch rate remains virtually constant for times lasting up to 90 min. The etch rate of $FeCl_3$ in a standing etchant is 1 μm/min for hole diameters ≥ 100 μm. The etch rate produced in the ultracentrifuge (−25,000g) was ≥ 40 μm/min for a hole diameter of 250 μm and 13 μm/min for a hole diameter of 100 μm.

With artificial gravity directed outward, we observed Bénard cell structures. Figure 7, which refers to a short etching time and therefore shallow etching, clearly shows the hexagonal structure characteristic of Bénard cells. This particular experiment was carried out in − 350g. The average size of the cell is about 100-200 μm. Smaller diameter holes etched under the same experimental conditions showed a similar cell pattern, the average cell size being again approxi-

Table II. Effect of gravity field and etching time on the etched depth (μm) of bronze; hole diameters: 100-1000 μm.

Artificial gravity	Etching time		
	7.5 min	15 min	60 min
+ 1g		20	
− 140g		100	100-300
− 350g	50	100	120-400
− 500g		125	160-400
−25,000g		200-400	

Table III. Average etch rate (μm/min). Etch depth (μm) per min for an artificial gravity of −350g; bronze.

Etching time used for averaging (in min)	Initial hole diameter (μm)			
	5000	500	250	100
7.5	17	7	6	8
30	13	3.5	3.5	2
60	7	3.5	3.5	2
90	4.5	3.5	3.5	2

Table I. Effect of gravity field on etched depth (μm) after 6 min etching of GaAs; hole diameter: 250 μm.

Etching time: 6 min	Etchant 5,5,2	Etchant 3,3,1
Standing etchant	6 μm	11 μm
+ 350g	25 μm	25 μm
− 350g	55 μm	50 μm

Fig. 7. Bénard cell structure (bronze, —350g); etching time, 15 min; etchant, FeCl₃; s.w., 1.35.

Fig. 9. Cellular pattern (OHW 350 μm. Bronze, —350g). Etching time: 1 hr; etchant: FeCl₃; s.w.: 1.39.

mately 100 μm, indicating that this is a length characteristic for the prevailing etching conditions. Although the hexagonal structure disappears as larger depths are reached, the cells remain, their appearance becoming more rounded. Smaller holes, with a diameter only a few times the characteristic length, exhibit a ring-like series of deep holes showing a pillar-like structure in the middle (Fig. 8-10). Below hole diameters of 150 μm, the multicell phenomenon disappears for reasons that should be obvious. Figure 11 shows a cylindrical hole of 100 μm diameter etched through a sheet that was 200 μm thick.

A simplified picture of the type of fluid flow that can be expected due to the Bénard phenomenon is shown in Fig. 4, where a linear array of Bénard cells is shown. Typically, the width and the height of a particular cell are of the same order of magnitude. The etch rate will be largest where downward directed fluid reaches the etchable surface. It will be lowest where the streamlines are directed away from the surface. Clearly, the etched cells will be approximately twice as large as the Bénard fluid cells. The ideal picture sketched in Fig. 3 refers to the case when exactly two Bénard cells fit into the cavity.

In the single experiment carried out at —25,000g, a similar cellular structure could be observed, although the phenomenon was not very distinctive. The cells appeared to have a diameter that was about one-quarter of those resulting from the —350g ex-
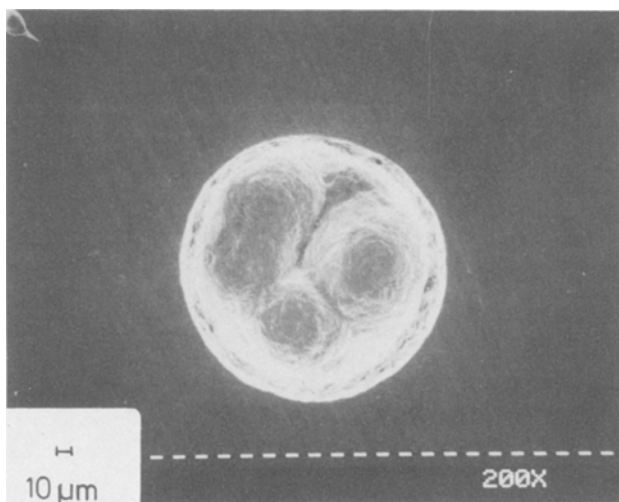

Fig. 10. Side view showing central pillar. Hole same as that of Fig. 9. (Bronze, —350g.)

Fig. 11. Cylindrical hole in bronze (width: 100 μm, depth: 200 μm, —350g). Etching time: 15 min; etchant: FeCl₃; s.w.: 1.35.

Fig. 8. Cellular pattern. Original hole width (OHW): 200 μm. (Bronze, —350g.) Etching time: 1 hr; etchant: FeCl₃; s.w.: 1.39.

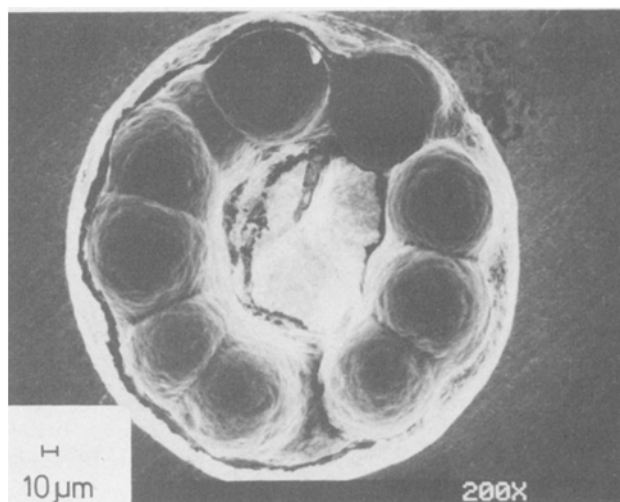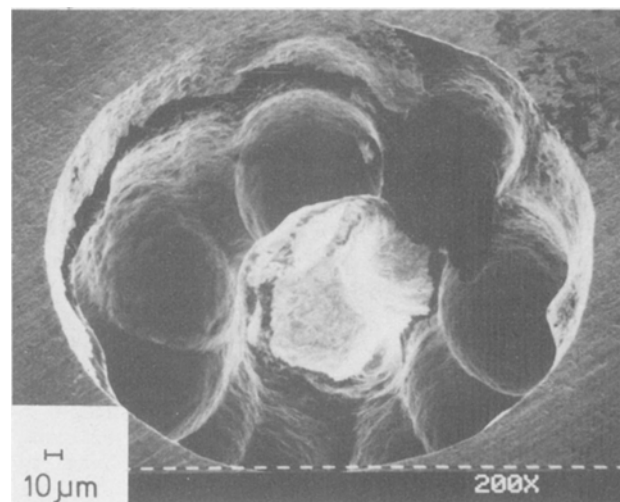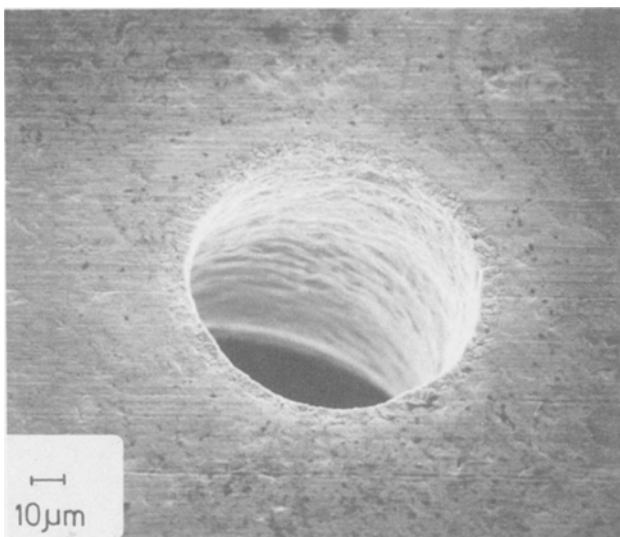periment. Figure 12 shows a hole with a diameter slightly larger than 100 μm. The bottom contains a great many cells; however the cells are rather vague. At — 350g, the same hole shows only a single cell
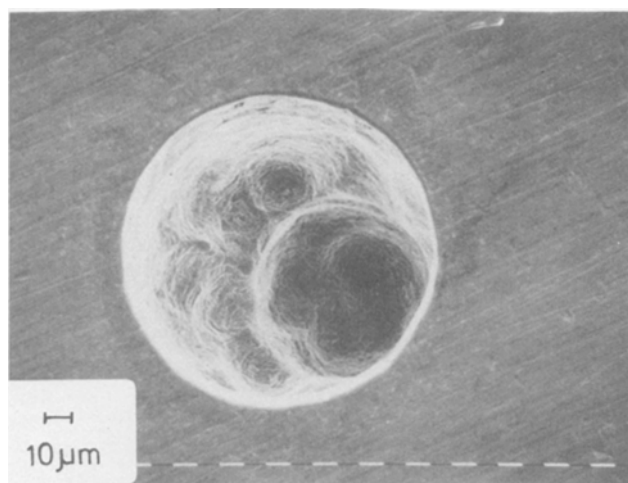
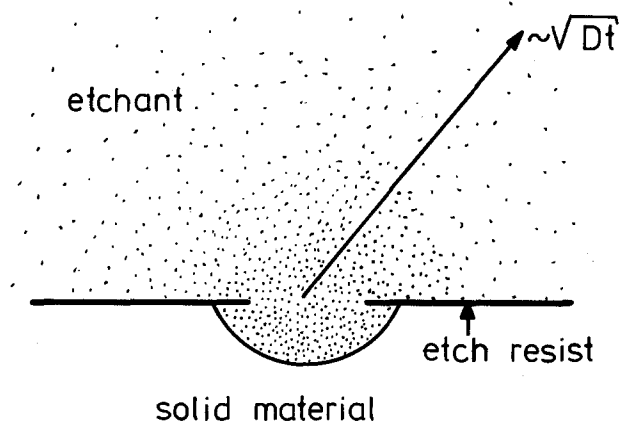Fig. 12. Cellular pattern at −25,000g (OHW 120 μm, bronze). Etching time: 15 min; etchant: FeCl$_3$.

Fig. 13. Diffusion field in a standing etchant. The density of the dots denotes the concentration level of reaction products. D is the diffusion coefficient and t is the time.
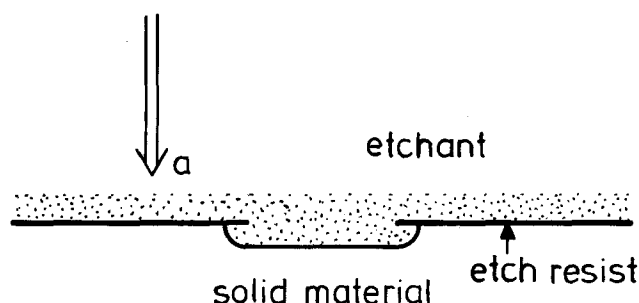

Fig. 14. The squeezing of reaction products against the substrate by means of an applied acceleration field a. It is assumed that reaction products are heavier than pure etchant.

and that would have filled the entire cavity. Pillar formation evidently depends upon the characteristic cell size; the larger the artificial gravity applied, the smaller the hole diameter is that reveals the phenomenon.

Despite these cells, the undercutting of the photoresist was very slight. When the sheets were etched through, no evidence of the cell structures was left, as the walls were smooth. Table IV gives a summary of the ratio of underetching to etched depth for various artificial gravities. This ratio appears to be independent of hole diameter. From the single experiment carried out in the ultracentrifuge, we tentatively conclude that the etch factor can even be much smaller under extreme acceleration conditions. At −25,000g, the etch factor appeared to be on the order of 0.05.

Although etch rate and undercutting seem to have a more or less regular behavior as a function of hole diameter and other parameters mentioned, it simply occurred too often to be considered accidental that, for hole diameters in the range 100-160 μm, the etch rate was clearly higher than that of both smaller and larger holes. In 15 min, we etched a hole 200 μm deep with a diameter of 100 μm holes. Holes of 400 μm deep with a diameter of 140-160 μm were etched in 30 min. The walls of these holes were as perfect as all the other holes obtained during the same experiments.

When holes had been etched through completely before etching stopped, an increase of the hole diameter occurred in the lower part of the holes. Figures 15 and 16, which refer to results obtained in the ultracentrifuge, clearly show this phenomenon.

Discussion

The experimental results presented in this exploratory paper clearly indicate that some remarkable results may be obtained by centrifugal etching. It would seem that relative etching depths can be reached that are simply not obtainable by the traditional methods of jet, spray, and film etching. The degree of undercutting is extremely low by ordinary standards. In many instances, our centrifugal etching

Table IV. Underetching—depth etching ratio for various artificial gravities and etching times: bronze.

Artificial gravity	Etching time		
	15 min	60 min	90 min
− 140g	0.13	0.13	
− 350g	0.13	0.12	0.10
− 500g	0.12	0.08	

procedure gave holes that were almost cylindrical, the etched depth being considerably larger than the final hole diameter. In an ultracentrifuge, etch rates may be achieved that are even larger than those obtained by ordinary jet etching methods. All these remarkable results were obtained when the artificial gravity was pointing away from the surface being etched.

Inward-directed artificial gravity.—On the other hand, when the acceleration field was pointing inward, extremely smooth surface finishes were seen. The etched bottoms were very flat, but now undercutting was not negligible. Still, the etch rate proved to be a fair bit higher than that obtained in a standing etchant. As an explanation, we might venture the following.

With inward directed artificial gravity, the reaction products are squeezed against the surface, the polluted layer becoming almost one-dimensionally stratified (Fig. 14). In the absence of the acceleration field, the etching products would have assembled in a semispherical slowly expanding diffusion region (Fig. 13), the thickness of which would be on the order of the diffusion length $(Dt)^{1/2}$. Since polluted etchant was assumed to be more dense than pure etchant, this semispherical region cannot be maintained in a force field that acts on the mass of a substance. Therefore, the polluted etchant will spread out over the surface which is "lowest" in the field, much as a layer of cold air would spread out over the surface of the earth. The one-dimensional stratification of the former case (with inward directed force field applied) leads to an effective diffusion length that is much smaller, where the diffusion length could be defined as the distance over which the concentration drops to 50% of its

highest value. As the etch rate is inversely proportional to the effective diffusion length, we may understand that etching will then proceed more rapidly. Evidence for this can be found in Table I where the application of a positive field led to an etch rate that was at least two times larger than that observed in a stationary etchant.

The smoothness of the surface finish observed in the positive, inward directed gravity case could be explained as follows. During etching, gaseous products may be created at the surface. In case these products are not dissolved completely, tiny gas bubbles will appear. If these remain attached to the wall, a coarse etched surface will be obtained. A strong positive field will pull these bubbles away from the surface the moment they appear, and a smoother etching process is obtained.

Bénard cells.—Returning now to the negative gravity case, it would seem that the most favorable conditions for fast deep etching exist when the hole diameter is just a little over the characteristic length given by the Bénard cell size. As we said before, for a given etching system, the cell size is fully determined by the magnitude of the artificial gravity. From the experiments on bronze in an FeCl$_3$ environment, performed at -350 and $-25,000g$, respectively, we found a reduction of the cell size from ~ 120 to ~ 30 μm. Since the etching systems were the same in the two cases, this means that the Ra number based on cell size (Eq. [2]) was the same in both experiments. Referring to the classical theories of Rayleigh-Bénard instability (14), we conclude that there is a critical Ra number at which convection sets in in a horizontally stratified fluid. This value of Ra is in the neighborhood of 1000. If this theory applies to the present case, we have a means of determining the correct acceleration needed to etch a given hole in an optimal sense. The required acceleration is

$$a = a_r (l_r/l)^3 \qquad [8]$$

where a_r and l_r are values obtained from an experiment that was carried out for reference purposes, and l is the given hole diameter. If Eq. [8] is applied to the two experiments mentioned earlier in this paragraph, we readily find that the values $a_r = 350g$, $a = 25,000g$, $l_r = 120$ μm, and $l = 30$ μm do satisfy Eq. [8] to a remarkable extent. Here it should be realized that the values of l_r and l were read directly from the photographs of Fig. 7 and 12 and are only correct in an approximate sense.

Etch rates: a comparison between theory and experiment.—We shall now investigate how the etch rates as shown in Table II can be explained with a view to the theoretical etch rates as expressed by Eq. [7]. In using Eq. [7], one should take into consideration that this equation is applicable only when the etching process has not yet proceeded to depths that are larger than the original width of the cavity. Indeed the experiments that led to Eq. [7] (13) were done on nonetchable stationary surfaces. When etching has proceeded to greater depths, the motive force attributable to free convection along vertical surfaces will dominate the etching process and a different (probably larger) Sh number will be obtained.

Another complicating factor that may hamper a correct judgment of the relative etch rates is to be found in the heat production that will occur during many etching processes. If the etchable area is much larger than the thickness of the sheet, the main part of the produced heat has to be carried off to the fluid, conduction through the sheet being only of minor importance. On the other hand, if the holes are relatively small, conduction may well be the main cooling factor, especially if the sheet material is a good heat conductor such as bronze. In the former case, only

one mode of heat transfer is present, and we may expect higher temperatures and consequently higher etch rates. Table III presents some evidence for this phenomenon, as the etch rate observed for the 5000 μm hole is significantly above that for the smaller holes.

With the provisos of the previous paragraph in mind, we may still attempt to explain the etch-depth variations presented in Table II. Since the Sh number is a measure of the ratio of the actual overall mass transport on the one hand and mass transport solely due to diffusion on the other, it will have a value of about one when stirring is absent or only very moderate. In Eq. [7a], we see that Sh is in the range of 3.5 to 6 when the Ra number varies in the range of 10^3-10^4. The etched depths given in Table II (15 min column) for the standing etchant and centrifugal ones of down to $-500g$ do seem to confirm this range of values. An estimate of the true value of the Ra number may be obtained as follows. As postulated above, in each centrifugal case, the value of Ra based on the width of the Bénard cell (half the width of the etched cell) is around 10^3. In the case of $-500g$, this size is $l_b \sim 60$ μm. For round holes, the Ra number of Eq. [7a] was based on the quarter-diameter (13). The Ra number can therefore be estimated as follows

$$Ra = 10^3 (l/4l_b)^3 \qquad [9]$$

where l is the diameter of the hole.

When comparing the etch rates obtained under different centrifugal conditions, one should be careful always to use holes of the same original diameter, since a rule such as Eq. [7a] gives the overall mass transfer from the hole. In actual fact, it is the mass-flow density (see Eq. [5]) that determines the etch rate. If we enter $L = l/4$ in [5], which is in accord with the conditions of Ref. (13), we may obtain from Eq. [7a] and [9]

$$\phi = 4.7 \, D \, (\Delta c) \, l^{-1/4} l_b^{-3/4} \qquad [10]$$

which shows a rather weak dependence upon the size of the cavity. The dependence upon l_b, the size of the Bénard cell, however, is rather strong. If two holes of the same size are etched with different centrifugal accelerations, the etch rate can be compared with the following rule

$$\phi_1/\phi_2 = [(l_b)_2/(l_b)_1)]^{3/4} = (a_1/a_2)^{1/4} \qquad [11]$$

where the last equality follows upon an application of Eq. [8]. If we apply Eq. [11] to the results presented in the 15-min column of Table II, taking the result for $-500g$ as a reference, we find an etched depth of 91 μm for $-140g$, 114 μm for $-350g$, and 330 μm for $-25,000g$. The observed values cannot be overly accurate, as it is impossible to define the exact depth of a cavity when the bottom is quite uneven. Nevertheless, there is a good correspondence between theory and experiment. In particular, it is satisfying to find that the depth predicted by Eq. [11] for $-25,000g$ is in the range of the observed values.

That the etch rate as expressed by Eq. [10] is only weakly dependent upon the width of the cavity, [*i.e.*, as long as the cavity is wider than $2l_b$] is an added advantage of the centrifugal etching technique over pure diffusion etching. In a standing etchant, the etch rate is dependent upon the initial size of the cavity, *i.e.*, the area of the etchable region. When the etched depth has become much larger than the initial hole diameter, the etch rate will have dropped to values that are much lower than those prevalent in the initial stages of the etching process. Obviously, this phenomenon will occur earlier when etching smaller holes. Therefore, a simultaneous etching of holes of different sizes may present problems if equal depths are required in the end. Jet etching, as we mentioned in
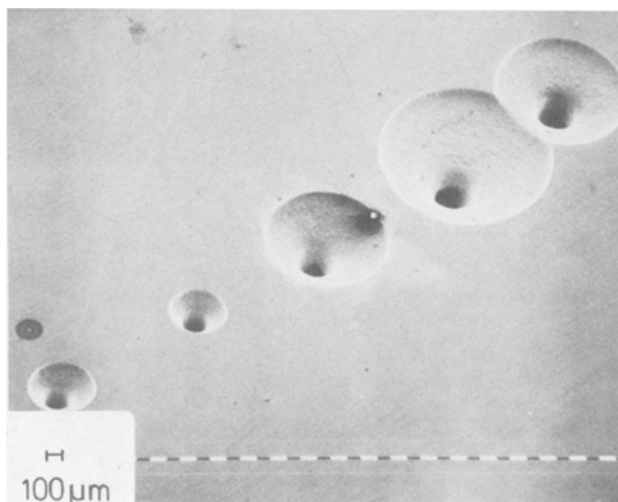
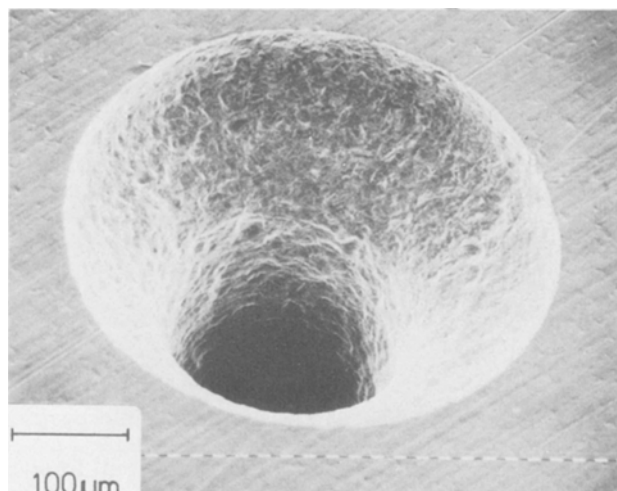Fig. 15. Abnormal etching at the underside after complete etch-through has occurred (bronze, —25,000g).

Fig. 16. Blow up of second cavity from the left in Fig. 15 (width: 400 μm; bronze, —25,000g).

the first section will also present problems here, as the etch rate will drop drastically when a depth comparable to the hole width has been reached. Centrifugal etching may offer a way out when care is taken that at least two Bénard flow cells fit into the smallest of the holes.

Abnormal etching after etch-through.—To explain the phenomenon shown by Fig. 15 and 16, we should realize the following. As soon as etch-through occurs, the concentration boundary layer acquires a definite leading edge. From the literature on boundary layers (1), we know that the largest normal gradients (for instance, that relating to mass transfer) occur at and

close to the leading edge. In our case, this must necessarily lead to a rapid sideways etching. This process clearly does not stop when the bottom has been etched away. Eventually, the shape of the sidewall will reflect the distribution of the mass transfer coefficient at the wall. Due to the special nature of this phenomenon, its occurrence is independent of the fact whether or not a photoresist layer covers the other side of the substrate. The only cause for its existence is that fresh etchant now hits the lower edge of the sidewall first. If the bottom is open, fresh etchant will be pulled in from behind the substrate. If a photoresist provides a permanent cover of the other side of the substrate, fresh etchant will be brought in through the orifice, then down through the center and along the photoresist cover toward the sidewall.

In conclusion, it is clear that our preliminary etching results do not give a complete picture of the capabilities of the centrifugal etching technique. Nevertheless, they do indicate that centrifugal etching can be a new and powerful tool in material technology.

Acknowledgment

REFERENCES

1. A. H. P. Skelland, "Diffusional Mass Transfer," Wiley-Interscience, New York (1974).
2. S. A. Trogdon and D. D. Joseph, *J. Non-Newt. Fluid Mech.*, **10**, 185 (1982).
3. H. K. Kuiken, *J. Eng. Math.*, **12**, 129 (1978).
4. G. Goosen and J. van Ruler, in "Proceedings of the World Conference on Metal Finishing," Interfinish, Amsterdam (1976).
5. D. M. Allen, D. F. Horne, and G. W. W. Stevens, *J. Photogr. Sci.*, **25**, 254 (1977).
6. D. M. Allen, D. F. Horne, and G. W. W. Stevens, *ibid.*, **26**, 72 (1978).
7. D. M. Allen, D. F. Horne, and G. W. W. Stevens, *ibid.*, **26**, 242 (1978).
8. D. M. Allen, D. F. Horne, and G. W. W. Stevens, *ibid.*, **27**, 181 (1979).
9. J. R. Selman and C. W. Tobias, *Adv. Chem. Eng.*, **10**, 212 (1978).
10. R. B. Bird, W. E. Stewart, and E. N. Lightfoot, "Transport Phenomena," Wiley, New York (1960).
11. V. G. Levich, "Physicochemical Hydrodynamics," Prentice Hall, Englewood Cliffs, NJ (1962).
12. A. A. Wragg, *Electrochim. Acta*, **13**, 2159 (1968).
13. R. J. Goldstein, E. M. Sparrow, and D. C. Jones, *Int. J. Heat Mass Transfer*, **16**, 1025 (1973).
14. S. Chandrasekhar, "Hydrodynamic and Hydromagnetic Stability," Clarendon Press, Oxford (1961).